Safety evaluation of magnetic catheter steering with upgraded magnetic resonance imaging system

G. Bringout *Student Member,IEEE*, V. Lalande *Student Member,IEEE*,
F.P. Gosselin and S. Martel *Senior Member,IEEE*

***Abstract*— Catheter navigation and placement through the arterial network is a major limitation for clinical procedure. In this article, a specific catheter tip and a modified clinical MRI scanner with an upgraded gradient system are used to steer a catheter through a single Y-shaped bifurcation. Safety aspects are analyzed to avoid the peripheral nerve stimulation (PNS) according to an empirical law of magnetostimulation and the magnetic field of upgraded 3D gradient coils. For a rabbit-sized device, the rising time of gradients system have to be limited to 1.7ms at 400$mT.m^{-1}$ to avoid PNS. These rise time values allow the use of this system for catheter steering and other more demanding applications.**

I. Introduction

CATHETER navigation through the body is a major limitation on several medical interventions, as catheters are placed and steered manually through a complex blood vessel network. Different solutions exist to improve catheter navigation. Stereotaxis, Sensei robotic catheter system and the CorPath System are clinical systems, but all of them use fluoroscopy to guide the catheter into the blood vessel network. Fluoroscopy uses ionizing radiations which may have serious health effects on the patient, physician and medical staff present during procedure in case of over-exposure. Compared with fluoroscopy, Magnetic Resonance Imaging (MRI) offers improved soft tissue resolution and eliminates ionizing radiation exposure [1]. Moreover, recent efforts [2], [3] have been put in to use the magnetic properties of the MRI apparatus for catheter manipulations. Using coils at the distal end of a catheter, different currents are applied to steer the tip of the catheter [2], [3]. Current is provided from a power supply or from the MRI radio-frequency subsystem. Other MRI subsystems can be used to steer objects inside the MRI bore. The main magnet of a typical MRI provides a permanent 1.5 T magnetic field at its center for imaging purpose. In addition, magnetic field gradients are generated in order to encode pixel/voxel locations of an observed volume. Recent works [4], [5] show that those two subsystems can be used to steer ferromagnetic objects. We propose to use the same method to steer a catheter tip which can be adapted on existing catheters.

This work is supported by a strategic grant from the Natural Sciences and Engineering Research Council of Canada (NSERC) and in part by a Canada Research Chair (CRC) in Micro/Nanosystem Development, Fabrication and Validation.

NanoRobotics Laboratory, Computer Engineering Department, Ecole Polytechnique Montreal (EPM), Montreal, Quebec, Canada, H3C 3A7. Corresponding author: Sylvain Martel, phone: 514-340-4711 ext:5098; e-mail: sylvain.martel@polymtl.ca

The catheter tip is made of a ferromagnetic sphere, which is magnetized in presence of the permanent magnetic field. Once magnetized, forces can be applied to the sphere with magnetic gradient field. Contrary to methods [2], [3], this method do not present risks of locally heating blood and tissue.

A clinical MRI system can typically generate 40$mT.m^{-1}$ gradient fields. However, steering applications require larger gradients field amplitudes [5]. In our steering application, a 400$mT.m^{-1}$ gradient field amplitude is used. This maximum amplitude is set as the technological limitations to scale up the coils to human size. To steer an object in 3D, three gradients coils are needed, one per direction. Using such high gradient amplitude is not directly a safety issue for in-vivo test. Safety limits come from time variation of magnetic fields. The risk is to stimulate nerves with quick magnetic field variations. Indeed, variations of magnetic fields in a time scale of milliseconds may induce a current inside the nerves of the patient. In the literature [6]–[11], the safety criteria for magnetostimulation take the form of limits on the absolute value of the time derivative of the magnetic field applied, dB/dt. High frequency imaging and steering gradients (see Fig. 1) imply high values of dB/dt which must be limited for safety reason. Commonly used dB/dt threshold values are based on human sized systems, with simplifications due to common size and designs of MRI gradient coils. As we intend to perform in-vivo tests on rabbits with custom gradient coils, the dB/dt threshold has to be reinterpreted according to this rabbit sized system.

The aim of the present theoretical study is to evaluate the feasibility of steering a magnetic catheter with a modified MRI apparatus while respecting safety limits with respect to magnetostimulation of an animal model (rabbit). In the first part of this paper, an accepted empirical law of magnetostimulation is applied on the theoretical model of an animal model to evaluate the threshold value of the dB/dt. Secondly, preliminary results on the steering of a magnetic catheter through a phantom are presented.

II. Stimulation thresholds

A. Theoretical model

1) Stimulations duration evaluation :dt value: Stimulation may occur when the gradient field amplitude change, due to the low rising time of the field, going from 0 up to 10ms [6]. The smaller the rising time value is, the higher are the risks of stimulation. In imaging procedure, a small rising time value is used to perform specific imaging tasks.

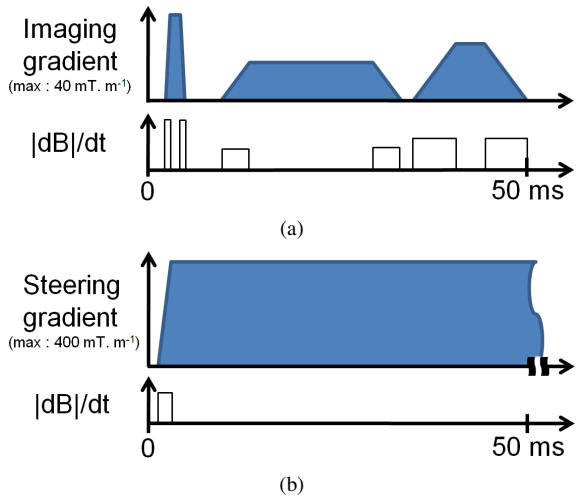

Fig. 1. Schematic representation of the time variations of gradient amplitudes in an MRI for imaging purposes (a) and for steering applications (b).

As the gradient field may switch every few milliseconds, the rising time value has to be minimized to maximize gradient field effect. Common MRI systems have a rising time values as small as $0.2ms$. The physical limitation on the minimum rise time of specific gradient system hardware comes from the coil inductance and the power supply maximum tension. When these two parameters are fixed, thus fixing the system minimum rising time value, any higher value can be generated with a specific power supply control.

2) PNS threshold determination: The PNS origin in MRI applications is an induced current from a tension field in a myelimated fibe [6], [7]. Different methods to evaluate the PNS threshold exist. The fundamental law of magnetostimulation [8] and Reillys exponential model [10] are two of them. Reillys model has show a good correlation with experimental data. The magnetostimulation law is based on the well established electrostimulation model [12], [13] and has shown a better correspondence with experimental data [8]. We choose to use the latter model for this better agreement.

The magnetostimulation law sets a PNS threshold defined as:

$$E_{stim} = rheobase(1 + \frac{chronaxie}{dt}). \quad (1)$$

E_{stim} is the tension field threshold ($V.m^{-1}$) above which peripheral nerves are stimulated by an induced current. The $rheobase$ ($V.m^{-1}$) is the low frequency limit of threshold stimulus. The $chronaxie$ (s) is the characteristic reaction time of the nerve. dt (s) is the duration of the stimulation pulse. Stimulation pulse occurs when gradients field vary from one value to another one, as shown in Fig. 1. According to (1), for a given dB, set by steering application, the dt (or rise time) is the only gradient system parameter which can be adapted to vary the stimulation threshold.

3) Induced electric Field amplitude calculation: The time variations of magnetic field B over a surface S and the electric field on the contour of that area are directly linked according to Maxwell-Faradays law:

$$\oint_{\partial S} \mathbf{E} \cdot d\boldsymbol{\ell} = -\iint_S \frac{\partial}{\partial t}\mathbf{B} \cdot d\mathbf{A}. \quad (2)$$

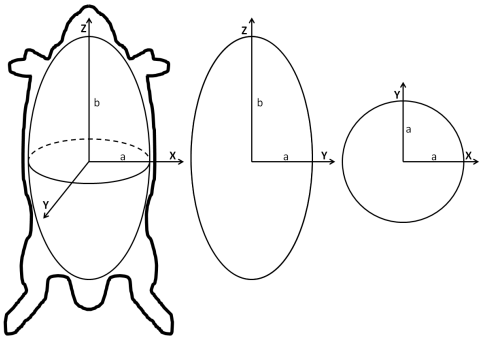

Fig. 2. Approximation of the volume of a rabbit by a prolate spheroid of homogeneous conductivity.

To simplify the evaluation of the induced electric field on the surface of a rabbit, we use conservative simplifying assumptions. First, we consider the volume of the rabbit as a prolate spheroid as shown in Fig. 2. Secondly, we take the magnetic field to be homogeneous and equal to its maximum value over the whole volume for each direction and coil [14]. And lastly, we concidere the electric field to be maximum when the magnetic field is maximum. Integrating (2) in each direction in space, we obtain :

$$|E_{XY}| = \frac{|B_Z|}{dt}\frac{a}{4}, \quad (3)$$

$$|E_{XZ}| = \frac{|B_Y|}{dt}\frac{ab}{2(3(a+b) - \sqrt{(3a+b)(a+3b)})}, \quad (4)$$

$$|E_{YZ}| = \frac{|B_X|}{dt}\frac{ab}{2(3(a+b) - \sqrt{(3a+b)(a+3b)})}, \quad (5)$$

where E_{XY}, E_{XZ}, E_{YZ} are the electrical fields ($V.m^{-1}$) induced around the XY, XZ and YZ surfaces of the rabbit by the B_Z, B_Y, B_X magnetic field (T), respectively. a (m) and b (m) are respectively the semi-minor and the semi-major axis of the ellipse, as shown in Fig. 2. Each gradient coil has three magnetic field components, as shown in Table I. The maximum induced field is reached when all three coils are at maximum amplitude. The maximum magnetic field amplitude is calculated from the sum of the maximum magnetic field of each coil ($w = x$, y or z) as :

$$B_{max} = \sqrt{(\Sigma B_{Xw})^2 + (\Sigma B_{Yw})^2 + (\Sigma B_{Zw})^2}. \quad (6)$$

The maximum surface of the spheroid cut by the plan perpendicular to the maximum magnetic vector, is an ellipse defined by the semi-minor and semi-major axes c and d. The equation of this ellipse can be obtained analiticaly or using CAD software. From equations (5) and (6) we define the maximum induced electric field E_{induce} ($V.m^{-1}$) on the prolate spheroid surface as:

$$E_{induce} = \frac{B_{max}}{dt}\frac{cd}{2(3(c+d) - \sqrt{(3c+d)(c+3d)})}. \quad (7)$$

TABLE I

VALUE OF MAXIMUM MAGNETIC FIELD FROM THE THREE DIFFERENT GRADIENT COILS, ACCORDING TO FIELD DIRECTION DEFINED IN FIG 2

		Gradient Coils		
		x	y	z
Field Direction	$\|B_X\|$	70mT	0mT	50mT
	$\|B_Y\|$	0mT	70mT	20mT
	$\|B_Z\|$	45mT	50mT	50mT

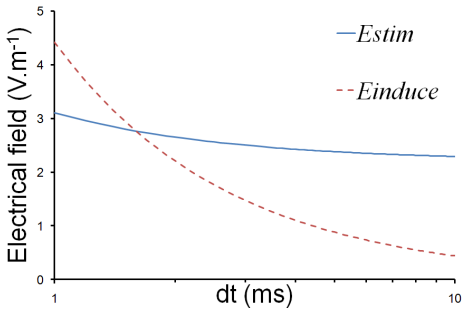

Fig. 3. Comparison of induced electric field in a rabbit body and the PNS threshold for a rabbit.

B. Results

To calculate the electric field threshold value, rabbit rheobase and chronaxie values have to be provided. In the literature, the only values we found for rabbits are $18.0V.m^{-1}$ for the rheobase and $0.41ms$ for the chronaxie [15]. We calculate a $12.2V.m^{-1}$ rheobase value from a different nerve model [16]. As those values show a significant variation, we decide to uses a $2.2V.m^{-1}$ rheobase which corresponds to the human value accepted by the international standard on MRI gradient safety [6], with a $0.41ms$ chronaxie, in order to provide a security factor of six. For the induced electric field, the typical lengths of the prolate spheroid are taken equal to $a = 0.065m$, $b = 0.280m$, $c = 0.065m$ and $d = 0.132m$. The maximum magnetic field produced by the 3D gradient coils are given in Table I.

In Fig. 3, electric field threshold values calculated from (1) and induced electric field values calculated from (7) are plotted against dt values. When the E_{induce} curve is above the E_{stim} curve, the induced current in the peripheral nerves is high enough to induce PNS. Otherwise, no PNS is generated. In Fig 3, the crossing point of the two curve shows that a dt of $1.7ms$ is sufficiently high to avoid any PNS in rabbits with 3D gradient coils. At $dt = 1.7ms$, to create a PNS, all 3D gradient coils have to be energized at the same time at maximum amplitude, i.e. $400mT.m^{-1}$. That represents a diagonal force direction on an application point having a nerve fiber parallel to the force direction.

This $1.7ms$ dt limit for a rabbit in gradient coils is easy to overcome and is compliant with the present application. This is also a strong result for other applications such as therapeutic magnetic micro carrier steering which require smaller dt value than catheter steering to be functional in a closed loop system. With the following experimental method, open loop catheter steering results are presented using a dt value of $10ms$.

III. CATHETER STEERING

A. Materials and Methods

1) Steering force: A steering force $\mathbf{F_{mag}}$ (N) applied to an object is proportional to the object volume V (m^3), magnetization M_Z ($A.m^{-1}$) and gradient of magnetic field $\nabla\mathbf{B_Z}$ ($T.m^{-1}$) applied on this object :

$$\mathbf{F_{mag}} = V M_Z \nabla \mathbf{B_Z}. \quad (8)$$

The volume of the ferromagnetic body which can be used is constrained by the purpose of the procedure and the object geometry. To avoid preferential magnetization direction due to the main magnetic field from the MRI, the object must have an isotropic shape such as a sphere.

The magnetization values depend on the material composition and on the magnetic field amplitude around the material. A 1.5T Sonata MRI scanner (Siemens AG, Germany) is used in this application and provides a 1.5T field that magnetizes most common ferromagnetic materials around 95% of their theoretical maximum value. Chrome steel spheres used in this application are ferromagnetic and have high magnetization saturation values. Finally, 3D gradient fields must be applied on the object to move it in space. Here, a single $400mT.m^{-1}$ pair of Maxwell coils are used to produce an external force on the catheter tip in only one direction. Hence, the sphere can only be steered in one direction.

2) Catheter steering: Experiments are performed with a FasTracker micro-catheter (Boston Scientific, USA), 2.5Fr (i.e.: $0{,}83mm$) external diameter with a bending rigidity evaluated at $1.2.10^{-6}N.m^2$. This measure was evaluated by measuring the bending induced by an end load. The catheter is clamped at a distance L of the distal tip in such a way as to avoid any rotation of the bending orientation. A soft ferromagnetic ball of chrome steel, $1.5mm$ diameter (Salemball, USA) and with a magnetization of $1\,248kA.m^{-1}$ in a 1,5T field (measured with a Vibrating Sample Magnetometer) is attached at the tip of the catheter. Experiments are conducted in a Y-shaped phantom and with a $90°$ angle between intersections (Fig. 4). The phantom and the catheter with the ball at the tip are placed in a bath of water to reduce the friction. The whole setup is placed in a 1-dimensional gradient coil inside the bore of a 1,5T MRI system. During the whole experiment, we move the clamp linearly along X, to simulate the action of the physician. As illustrated in Fig. 4 we define X as the direction parallel to the catheter and Z as the direction perpendicular to catheter and parallel to the main MRI magnetic field. Without any gradient applied, we observe the intersection naturally chosen by the catheter inside the phantom due to its natural bending. Once this preferred direction (PD side) is known, we apply the gradient field in the opposite direction (OD side). The amplitude of the gradient is varied from 0 to $400mT.m^{-1}$ by $11mT.m^{-1}$ increments and then from 400 to $0mT.m^{-1}$.

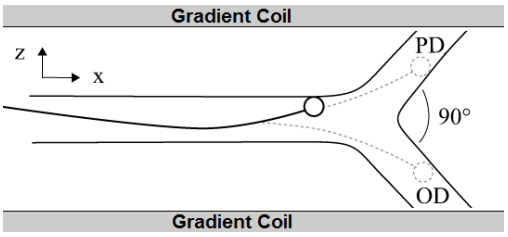

Fig. 4. Schematic representation of the phantom and the catheter-ball.

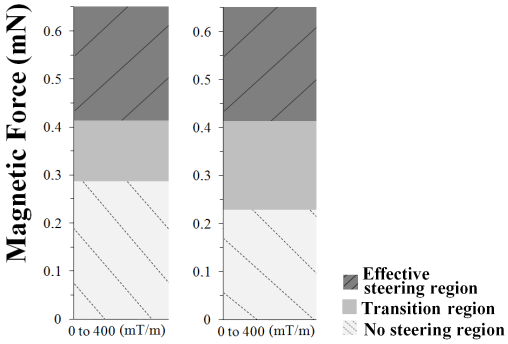

Fig. 5. Efficacy of steering of the catheter in the experiments of varying magnetic loading. (a): the loading cycle. (b): the unloading cycle.

B. Results

Steering results are plotted in Fig. 5. Three different regions are shown: a no steering region during which the gradient application amplitude does not induce a magnetic force sufficient enough to counter the natural behavior; the catheter tip still goes to the PD side. An efficient steering region defined by the catheter tip being effectively steered in the OD with the gradient. Finally, a transition region while the catheter bumps into the middle of the intersection and buckles when pushed forward.

The left hand side bar plot of Fig. 5 shows the required magnetic force for steering for an increasing magnetic load (0 to $400mT.m^{-1}$) while on the right hand side is shown that for unloading (400 to $0mT.m^{-1}$).

The efficient steering region starts with the same force application. However, the transition region lasts longer for the test starting at $400mT.m^{-1}$. This phenomenon is due to the coercitivity of the material which tends to stay magnetized.

IV. Discussions and conclusion

With those custom gradient coils, the power supplies and the control algorithm have to be carefully chosen to have a rise time value always superior to $1.7ms$. It has been shown that this limit is very conservative for the use on rabbits and permits to steer a catheter tip inside a Y-shaped phantom. Furthermore, the $400mT.m^{-1}$ gradient amplitude limitation of the system leaves a margin to steer catheter through more complex intersections.

For human sized steering coil, dB/dt calculations must be adapted. As the dimensions of the prolate spheroid increases, the induce electric field increase. To avoid to be above the PNS threshold and to keep a low dt value, we first have to do more precise calculations of the induced electric field. Moreover, as high values of magnetic fields are only present near gradient coils surfaces, technical solutions exist to reduce the maximum amplitude of magnetic field on the coil surface and thus decrease the dt value without affecting performances.

V. Acknowledgments

Authors acknowledge the help of Pr Pierre Savard (EPM) in magnetostimulation, Pierre Pouponneau (EPM), Jean-Baptiste Mathieu (EPM) and Charles Tremblay (EPM) for discussions.

References

[1] S. Nazarian, A. Kolandaivelu, M. Zviman, G. Meininger, R. Kato, R. Susil, A. Roguin, T. Dickfeld, H. Ashikaga, H. Calkins *et al.*, "Feasibility of real-time magnetic resonance imaging for catheter guidance in electrophysiology studies," *Circulation*, vol. 118, no. 3, p. 223, 2008.

[2] F. Settecase, M. Sussman, M. Wilson, S. Hetts, R. Arenson, V. Malba, A. Bernhardt, W. Kucharczyk, and T. Roberts, "Magnetically-assisted remote control (MARC) steering of endovascular catheters for interventional MRI: A model for deflection and design implications," *Medical physics*, vol. 34, p. 3135, 2007.

[3] N. Gudino, "Control of Intravascular Catheters Using a 3D Array of Active Steering Coils for and Interventional MRI setting," 2008.

[4] P. Pouponneau, J. Leroux, and S. Martel, "Magnetic nanoparticles encapsulated into biodegradable microparticles steered with an upgraded magnetic resonance imaging system for tumor chemoembolization," *Biomaterials*, 2009.

[5] J. Mathieu and S. Martel, "Magnetic microparticle steering within the constraints of an MRI system: proof of concept of a novel targeting approach," *Biomedical Microdevices*, vol. 9, no. 6, pp. 801–808, 2007.

[6] I. E. Commission, "Medical electrical equipment. Part 2. Particular requirements for the safety of magnetic resonance equipment for medical diagnosis. International Standard 60601-2-33," 2008.

[7] J. Schenck, W. Edelstein, H. Hart, C. Williams, C. Bean, P. Bottomley, and R. Redington, "Switched gradients and rapidly changing magnetic-field hazards in NMR imaging," *Med. Phys*, vol. 10, pp. 133–133, 1983.

[8] W. Irnich and F. Schmitt, "Magnetostimulation in MRI," *Magnetic Resonance in Medicine*, vol. 33, no. 5, pp. 619–623, 2005.

[9] B. Recoskie, T. Scholl, and B. Chronik, "The discrepancy between human peripheral nerve chronaxie times as measured using magnetic and electric field stimuli: the relevance to MRI gradient coil safety," *Physics in Medicine and Biology*, vol. 54, p. 5965, 2009.

[10] J. Reilly, "Peripheral nerve stimulation by induced electric currents: exposure to time-varying magnetic fields," *Medical and Biological Engineering and Computing*, vol. 27, no. 2, pp. 101–110, 1989.

[11] J. Reilly, V. Freeman, and W. Larkin, "Sensory Effects of Transient Electrical Stimulation Evaluation with a Neuroelectric Model," *IEEE Transactions on Biomedical Engineering*, pp. 1001–1011, 1985.

[12] G. Weiss, "Sur la possibilité de rendre comparables entre eux les appareils servant à l'excitation électrique," *Arch Ital Biol*, vol. 35, pp. 413–46, 1901.

[13] L. Lapicque, "Définition expérimentale de l'excitation," *Comptes Rendus Acad Sci Paris*, vol. 67, no. 2, pp. 280–283, 1909.

[14] J. Reilly, "Magnetic field excitation of peripheral nerves and the heart: a comparison of thresholds," *Medical and Biological Engineering and Computing*, vol. 29, no. 6, pp. 571–579, 1991.

[15] M. Yamaguchi, S. Yamada, N. Daimon, I. Yamamoto, T. Kawakami, and T. Takenaka, "Electromagnetic mechanism of magnetic nerve stimulation," *Journal of Applied Physics*, vol. 66, p. 1459, 1989.

[16] B. Roth and P. Basser, "A model of the stimulation of a nerve fiber by electromagneticinduction," *IEEE Transactions on Biomedical Engineering*, vol. 37, no. 6, pp. 588–597, 1990.